RSC Advances

PAPER

View Article Online
View Journal | View Issue

Cite this: *RSC Adv.*, 2014, **4**, 2103

Spatiotemporal effects of a bioautocatalytic chemical wave revealed by time-resolved mass spectrometry†

Hsu Ting[a] and Pawel L. Urban*[ab]

Received 10th June 2013
Accepted 30th October 2013

DOI: 10.1039/c3ra42873g

www.rsc.org/advances

Mass spectrometry has been implemented as an on-line detection tool to monitor transmission of chemical signals due to natural processes such as diffusion and convection as well as a bienzymatic autocatalytic process. It was found that the enzyme-accelerated chemical wave propagates faster than the chemical wave propelled by other processes. The two enzymes (pyruvate kinase and adenylate kinase), involved in the process, work co-operatively catalysing production of adenosine diphosphate (ADP) and adenosine triphosphate (ATP), and induce formation of a front propagating along a high-aspect-ratio drift cell towards the ion source of an ion trap mass spectrometer. Isotopically labelled ^{13}C-ATP was used as the trigger of the accelerated chemical wave. Using this substrate, one could easily distinguish between the two chemical waves (passive and accelerated) in a single experiment, reducing the bias due to the inherent experimental instabilities. We think that – following further improvements – the process described in this report may find applications in bioengineered systems, in which chemical signals need to be transmitted over macroscopic distances.

1. Introduction

In nature, diffusion and convection are responsible for translocation of chemical molecules over micro- and macro-scopic distances. Diffusion uses internal energy to equalize concentrations of substances in the surrounding space, while convection is responsible for collective movement of molecules in a field gradient. Both processes underlie interactions occurring between chemical molecules. They ascertain mixing of substances in chemical reactors, and enable communication between cells in tissues.[1] In various components of biomolecular machinery, a faster transport (or chemical signal transduction) is required than that provided by diffusion and convection. Nature has invented efficient ways of transmitting molecules and chemical signals, which are faster than those enabled by diffusion and convection. For example, proteins are actively moved within biological cells along the fibres of cytoskeleton, so that they can be delivered quickly to specific locations.[2] In artificial systems, diverse pumping methods are used: for example, hydrodynamic[3] or electroosmotic[4] flow can be exerted on a fluid by using a syringe pump or an electrical power supply, respectively. It is also known that reaction-diffusion systems lead to formation of moving fronts.[5,6] They are driven by the difference between the chemical potentials of the reactants and the products. Other studies also revealed that even common chemical reactions – such as acid–base neutralization – can produce hydrodynamic instabilities,[7] inducing macroscopic movements of chemical molecules. Due to the growing interest in bioengineering, it would be desirable to possess a method of transmitting chemical signals over macroscopic distances – in a controlled manner – without the reliance on mechanical or electrical devices, which would be compatible with biochemical systems. A suitable candidate for such a method would be an enzymatic autocatalytic process.

Here we describe a semi-artificial chemical process incorporating a bienzymatic reaction, which is capable of generating chemical waves that propagate over macroscopic distances in a liquid medium at room temperature – faster than diffusion and convection. It is based on a bienzymatic reaction system[8,9] using adenosine diphosphate (ADP) and adenosine triphosphate (ATP) as the carriers of chemical signal:

$$\mathrm{ATP} + \mathrm{AMP} \xrightarrow{\text{adenylate kinase}} 2\mathrm{ADP} \quad (1)$$

$$\mathrm{ADP} + \mathrm{PEP} \xrightarrow{\text{pyruvate kinase}} \mathrm{ATP} + \mathrm{PR} \quad (2)$$

According to the above scheme, ATP is the substrate in reaction (1) and the product of reaction (2). Conversely, ADP is the substrate of reaction (2) and the product of reaction (1). The key feature of this autocatalytic system is that, in reaction (1), 2 molecules of ADP are synthesized out of one molecule ATP. This subsequently doubles the number of ATP molecules produced

[a]*Department of Applied Chemistry, National Chiao Tung University, Hsinchu 300, Taiwan. E-mail: plurban@nctu.edu.tw*

[b]*Institute of Molecular Science, National Chiao Tung University, Hsinchu 300, Taiwan*

† Electronic supplementary information (ESI) available: Additional figures. See DOI: 10.1039/c3ra42873g

in reaction (2). Hence, the number of cycling ADP and ATP molecules will double in each sequence, while the co-substrates (adenosine monophosphate (AMP) and phosphoenolpyruvate (PEP)) are consumed, and a by-product (pyruvate, PR) is formed. Since none of the products of reactions (1) and (2) absorb light in the visible part of electromagnetic spectrum, it is not easy to follow spatiotemporal characteristics of the process. Therefore, in order to demonstrate the concept outlined above, we implemented a time-resolved mass spectrometry[10] approach, which enabled monitoring of the non-chromogenic ionisable reactants in real time, and with an adequate temporal resolution. In fact, time-resolved mass spectrometry offers important advantages in such experiments because: fast-changing reactants of an autocatalytic process can be monitored with minimum cross-interferences; with high selectivity, sensitivity, and speed.

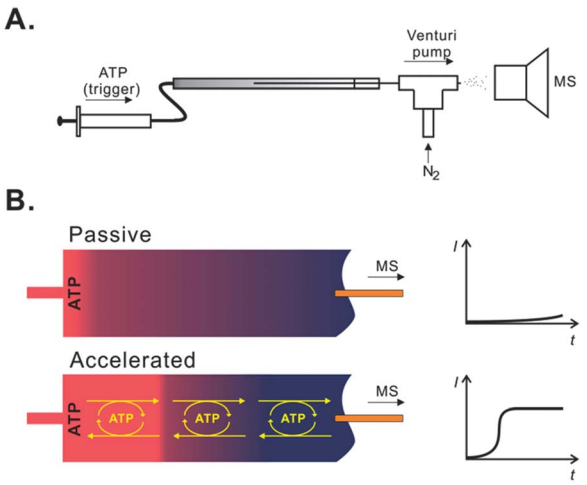

Fig. 1 Investigation of a chemical wave due to "passive" transduction and bienzymatic amplification system (eqn (1) and (2)). (A) Experimental setup incorporating a horizontal drift cell and mass spectrometer. (B) Schematic representation of chemical wave propagation in the drift cell due to the passive and the enzyme-accelerated transduction.

2. Experimental section

2.1. Materials

Ammonium acetate, adenosine 5′-monophosphate monohydrate (AMP), adenosine 5′-triphosphate disodium salt hydrate (ATP), adenosine-$^{13}C_{10}$ 5′-triphosphate sodium salt solution ($^{13}C_{10}$-ATP), ethylenediaminetetraacetic acid (EDTA) tetrasodium salt dihydrate, potassium chloride, and magnesium sulphate were from Sigma-Aldrich (St Louis, USA). Phosphoenolpyruvic acid monopotassium salt was from Alfa Aesar (Ward Hill, USA). The two enzymes – adenylate kinase (myokinase from chicken muscle, catalogue no. M5520, essentially salt-free, lyophilized powder, 1500–3000 units mg^{-1} protein) and pyruvate kinase (from rabbit muscle, catalogue no. P9136, type III, lyophilized powder, 350–600 units mg^{-1} protein) – were from Sigma-Aldrich. On arrival, the enzymes were dissolved in 1 mL 10^{-2} M ammonium acetate to reach the specific activities of 1000 U mL^{-1}. The fused silica capillary with the ID 150 μm (OD 375 μm) – used in the Venturi pump assembly – was obtained from GL Science (Tokyo, Japan).

2.2. Apparatus and procedure

In the beginning of the experiment, the drift cell (standard NMR tube with perforated bottom) was filled with a solution of enzymes, the main substrates (except ATP), cofactors, and buffer components (Fig. 1A). The composition of the reaction medium was: 10 mM ammonium acetate, 0.1 mM EDTA, 0.1 mM potassium chloride, 0.1 mM magnesium sulphate, 0.1 mM AMP, 0.1 mM PEP, 5 U mL^{-1} pyruvate kinase, and 5 U mL^{-1} adenylate kinase. In the experiment involving demonstration of accelerated transduction, adenylate kinase was added to the reaction mixture right before loading the drift cell. In the experiment involving demonstration of passive transduction, adenylate kinase was not included in the medium, so the cycling reaction (eqn (1) and (2)) could not proceed. Special precautions were taken to prevent introduction of air bubbles. The drift cell was placed horizontally in a holder attached to an *xyz*-stage located in front of the mass spectrometer. Fused silica capillary (ID 150 μm, OD 375 μm) attached to Venturi pump[11] (1/8-inch stainless steel tee; Swagelok, Supelco; Solon, OH, USA) was inserted into the drift cell, so that the distance between the inlet of the drift cell, and the inlet of the fused silica capillary, was ~4 cm. While the outlet of the drift cell was open, the inlet was hydraulically connected to a 100 μL glass syringe filled with the ATP solution (also containing the buffer components as for the enzymatic reaction). The reaction solution was held inside the open tube due to cohesive and adhesive forces. Nitrogen gas was supplied to the Venturi pump (pressure: ~207 kPa) in order to induce suction of the liquid sample, nebulisation, and ionisation of the analytes in front of the orifice of the mass spectrometer. The flow rate of the sample solution in the fused silica capillary was ~840 μL h^{-1}. Such low flow rate does not produce significant advective movement of the solution inside the drift cell. It is predicted that much of the liquid aspirated by the Venturi pump originates from the section of drift cell downstream from the inlet of the fused silica capillary (closer to the open end of the drift cell), and a small fraction of the aspirated liquid comes from the end section of the 4 cm long drift region. After setting up the drift cell, data acquisition was started, and the syringe pump was set to inject 30 μL of the ATP solution with the flow rate of 20 μL min^{-1}. Following the injection of the trigger ATP – which took 90 s – the syringe pump was on stand-by.

In order to monitor the propagation of chemical waves (either due to classical phenomena or accelerated transduction of chemical signals) we used an ion trap mass spectrometer (amaZon speed; Bruker Daltonics, Bremen, Germany) operated in the negative-ion mode. The voltage applied to the ion transfer capillary was 2500 V, and the end-plate offset was set to 500 V. The flow rate of the dry gas was set to 6.5 L min^{-1}. The mass range was set to 15–700 u e^{-1}. The data were collected with TrapControl software (ver. 7.1; Bruker Daltonics), exported to ASCII files, and further treated in Excel (2010; Microsoft, Redmond, WA, USA).

3. Results and discussion

3.1. Verification of wave propagation

In order to verify the possibility of transmitting chemical signals (ADP/ATP) over a macroscopic distance, we used a simple experimental setup (Fig. 1A) comprising a horizontal tube with a high aspect ratio (drift cell) with inlet and outlet ports. The drift cell was filled with the mixture of all the reactants and enzymes required for the bienzymatic process (reactions (1) and (2)) except for ADP and ATP. The outlet port of the drift cell was connected to the Venturi pump[11] providing a constant but relatively low suction force. The reaction solution was constantly probed, and transferred to the ionization zone of the ion trap mass spectrometer. The inlet port of the drift cell was connected to a syringe filled with ATP solution. A small aliquot of ATP solution (~30 μL) was dispensed in order to trigger the chemical wave. The chemical wave propagated over the distance of ~4 cm – measured from the inlet port of the drift cell to the inlet of the capillary incorporated into the Venturi pump assembly (Fig. 1A and S1†). Importantly, the volume of this 4 cm long section corresponds to ~600 μL. Thus, the injection of 30 μL ATP solution (~5% of the drift volume) has negligible contribution to advective motion inside the drift cell.

Fig. 1B illustrates two alternate schemes of the propagation of chemical wave in the drift cell, based on passive (top) and accelerated (bottom) transduction. We hypothesized that chemical wave carried by the enzymatic reactions in (1) and (2) will transmit the ATP signal towards the outlet port of the drift cell faster than passive transduction due to diffusion and convection along with the advective motion induced by the Venturi pump. An initial hypothesis was that the reactions (1) and (2) can rapidly elevate local concentration of ADP/ATP as soon as a small amount of these species is brought to an ADP/ATP-free region of the reaction medium. Therefore, convection, advection and diffusion would only be needed to propel the chemical wave in microscale, while the autocatalytic reaction system would accelerate its propagation along the drift volume. This hypothesis was verified using time-resolved mass spectrometry as a tool of chemical analysis in real time. To simplify evaluation of the mass spectrometric data, the signal intensities (I, sum of signal intensities across a short section of mass spectrum near the peak centroid, ±0.5 u e^{-1}) corresponding to the signals of AMP, ADP, and ATP (*cf.* Fig. S2†) were computed according to the formula:

$$\text{Rel. yield} = \frac{I_{\text{ADP}} + I_{\text{ATP}}}{I_{\text{AMP}} + I_{\text{ADP}} + I_{\text{ATP}}} \quad (3)$$

smoothed, and plotted against time (Fig. 2). The reaction was run with an optimized and characterized composition of the reactant mixture (*cf.* Fig. S3†). In Fig. 2, one can clearly see the difference between the two cases corresponding to the passive and the accelerated transduction, respectively. The upper graph in Fig. 2 shows the result of an experiment in which adenylate kinase was not included in the reaction cocktail. Therefore, the cycling bienzymatic reaction did not occur. The bottom graph in Fig. 2 shows the result of an experiment in which both enzymes were present in the reaction cocktail. In the former case, the propagation of ATP was mainly due to convection and diffusion, superimposed with the advective motion arising in the drift cell (passive transduction). In the latter case, amplification of ATP could take place. Therefore, the fast appearance of ATP is attributed to the bienzymatic reaction which increases local concentration of ATP – provided that a small amount of ATP is available to trigger the cycling process (accelerated transduction). This result confirms the hypothesis illustrated in Fig. 1B showing the feasibility of using the bienzymatic system in (1) and (2) to propagate a chemical wave with a speed higher than it would result from the classical mass transport (Fig. 1A).

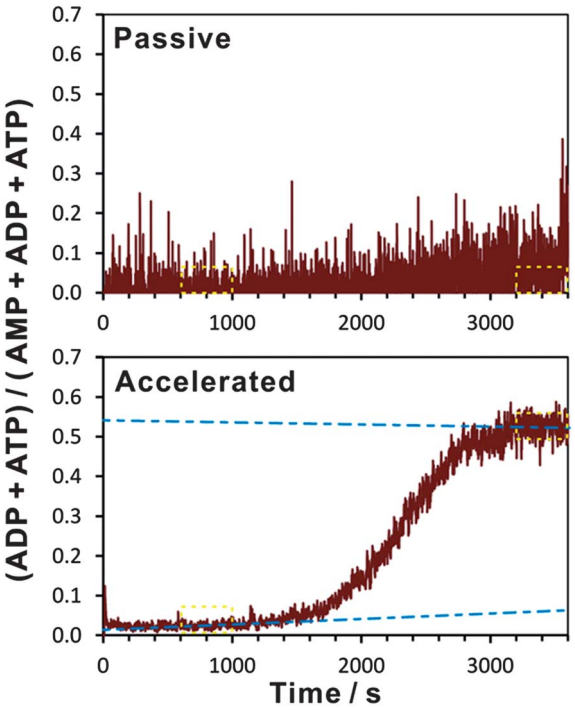

Fig. 2 Propagation of a bioautocatalytic chemical wave in a horizontal drift cell, recorded online by time-resolved mass spectrometry: passive (top) *vs.* accelerated transduction (using the bienzymatic reaction system; bottom). Concentration of the trigger ATP: 5×10^{-3} M. Fig. S4† presents unprocessed extracted ion currents from this experiment. Exponential smoothing with a time constant of 4.1 s has been applied. Yellow dashed frames indicate the time ranges for which average relative intensities were calculated (see the narrative text for explanation). Blue dashed lines are linear functions fitted to the datasets highlighted with yellow dashed frames to facilitate visual assessment.

The ratios of the relative yield in the end of the run (3200–3600 s) to the relative yield in the beginning of the run (600–1000 s; *cf.* yellow dashed frames in Fig. 2) were 4.5 and 21.4, in the case of passive and accelerated transduction, respectively (values calculated without prior normalization of datasets). This shows a relative gain of the chemical signal corresponding to an elevated concentration of ADP and ATP. These differences are also visible in the unprocessed extracted ion currents (Fig. S4†). While the result in Fig. 2 (top, passive transduction) exhibits an elevation of trace at the end of the run, the exact timing of the arrival of chemical wave in this experiment was not perfectly

reproducible. This is because the liquid inside drift cell is not perfectly quiescent. The temperature gradient in front of the mass spectrometer, and the hydrodynamic flow exerted by the Venturi pump used for ionization, induce advective movements inside the tube. Formation of local eddies – near the inlet of Venturi pump capillary – can lead to chaotic mixing inside the drift cell and instabilities of the MS signal. Instabilities of experimental conditions (*e.g.* occurrence of temperature gradient in front of MS, decay of enzymatic activity) may be responsible for unsatisfactory reproducibility of the obtained results. Therefore, comparison of the results can only be valid if the two experiments (involving passive and accelerated transduction) are carried out in a series – using the same setup and conditions. We tried to assure this as much as possible but also sought another dependable method to investigate the enzyme-accelerated chemical waves.

3.2. Implementation of an isotopically labelled trigger

In order to provide a solid evidence for the higher speed of enzyme-accelerated transduction relative to passive transduction – and overcome the reproducibility problems mentioned above – we subsequently implemented isotopically labelled ATP as a trigger of the chemical wave. When 30 μL $^{13}C_{10}$-ATP is injected to the inlet port of the 600 μL section of the drift cell, it initiates the bienzymatic autocatalytic process. However, since the substrate AMP (0.1 mM) contains ^{12}C isotope, the newly produced ADP and ATP molecules are not labelled. Thus, we can consider the chemical wave produced by the reaction as a carrier of unlabelled ADP and ATP. The labelled $^{13}C_{10}$-ATP migrates mainly due to passive transduction (convection, diffusion, advection), and its role as the reaction trigger ceases as the populations of the newly synthesized unlabelled ADP and ATP molecules grow. In this experiment, following the injection of 10^{-2} M $^{13}C_{10}$-ATP, the two waves – corresponding to unlabelled and labelled ADP/ATP species – were recorded. Experimental data were treated according to the following formulae:

$$\text{Rel. yield } (^{12}C) = \frac{I_{ADP} + I_{ATP}}{I_{AMP} + I_{ADP} + I_{ATP} + I_{13CAMP} + I_{13CADP} + I_{13CATP}} \quad (4)$$

and

$$\text{Rel. yield } (^{13}C) = \frac{I_{13CADP} + I_{13CATP}}{I_{AMP} + I_{ADP} + I_{ATP} + I_{13CAMP} + I_{13CADP} + I_{13CATP}}, \quad (5)$$

smoothed, normalized, and displayed in time domain (Fig. 3). The normalization was done by scaling the values of the datapoints to the maximal value within the displayed time range. Interestingly, even at the high concentration of the trigger ATP (10^{-2} M), a difference in the propagation speed could be observed (Fig. 3, top). In this particular experiment, accelerated transduction led to a sharp increase of the signal (blue trace), whilst passive transduction of labelled ATP led to a gradual increase of the ionisable species (red trace). At a lower concentration of the ^{13}C-ATP, used as the trigger, the edges of

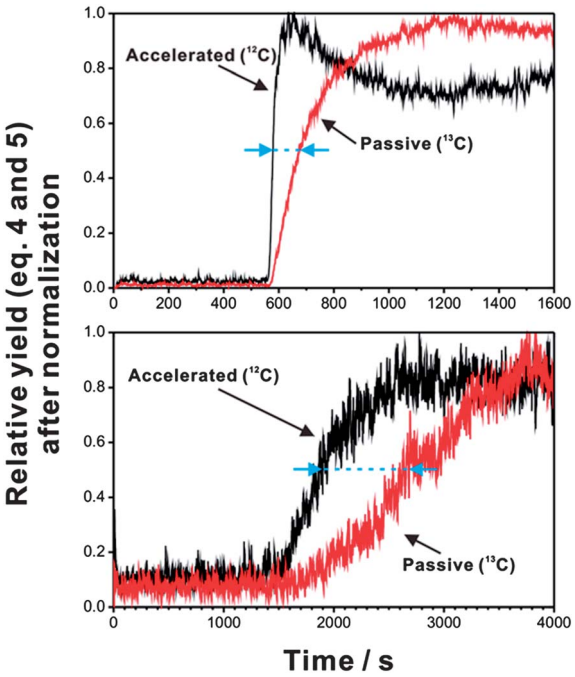

Fig. 3 Transduction of labelled and unlabelled ATP along the drift cell. Concentration of the $^{13}C_{10}$-ATP trigger: 10^{-2} M (top) and 5×10^{-3} M (bottom). See Fig. S5† for replicates of the concentration 5×10^{-3} M. Fig. S6† presents unprocessed extracted ion currents from the experiment with the concentration 5×10^{-3} M. Exponential smoothing with a time constant of 4.1 s has been applied, and followed by normalization (scaling to the maximal value). Dashed blue line denotes the time lapse between half-maxima of the normalized curves (0.5 level) corresponding to the passive and accelerated chemical transduction: 93 and 740 s in the case of 10^{-2} M and 5×10^{-3} M trigger solution, respectively.

the accelerated and the passive fronts were less sharp (Fig. 3, bottom) but the difference between half-maxima of the normalized profiles was greater: 740 *vs.* 93 s in the case of 5×10^{-3} and 10^{-2} M trigger, respectively (Fig. 3). The differences between the accelerated and the passive transduction could be observed in all the replicate experiments using isotopically labelled trigger (Fig. S5†) even though both fronts shifted due to the above-mentioned imperfections of the experimental setup. Based on this, one may conclude that – in the present experimental setup – the onset of the increase is determined by the advective transport, and the chemical wave has a relatively small influence when compared with the advection. It is also worthwhile noting that the inspection of the unprocessed datasets also led to the observation of a higher speed of the bio-autocatalytic chemical wave, as compared with the passive transduction (Fig. S6†). Nonetheless, the difference is less evident than in the plot of the processed data (Fig. 3).

3.3. Final remarks and outlook

The results presented above highlight the possibility of using enzyme-aided chemical waves as a means to transmit binary signals. However, to increase practicality of this scheme, one may consider incorporating a "quenching" mechanism, so that

the system can return to its initial state (low level of ADP and ATP in the drift cell). This might be achieved by incorporating a mechanism to hydrolyze ADP and ATP to AMP once the signal reaches the outlet end of the drift cell. It is also worthwhile noting that the experiment using the isotopically labelled trigger ATP does not require additional control because spatiotemporal behaviour of two populations of ATP are recorded in one run.

It was previously reported that hydrodynamic instabilities can be induced by chemical reactions, and subsequently influence convective motion.[7] The current experimental model shows that a chemical reaction itself can produce an apparent "motion" of reactant molecules, which does not seem to be directly connected with advection (that certainly exists in the current experimental system).

Chemical waves are often discussed in the context of oscillating reactions, with the most prominent example being the Belousov–Zhabotinsky reaction,[12] which produces oscillating chemical waves composed of iron complexes and other species. Unlike Belousov–Zhabotinsky reaction, the chemical wave reported here has a character of a moving front of elevated concentration, without apparent oscillations (except those attributed to imperfections of the experimental setup and formation of eddy currents). The proposed system is suitable for operation at the room temperature. In addition, unlike many oscillating reaction schemes, the system reported here uses an aqueous buffer at neutral pH, which renders it biocompatible. We believe more chemical wave reaction schemes can be demonstrated in future, for example, implementing various ways of molecular amplification. However, not every amplification reaction can offer the advantage of sending a chemical signal in a seamless fashion. For instance, the most famous one – polymerase-chain reaction (PCR)[13] – requires periodic changes of temperature, which certainly eliminates the advantage of sending chemical signals without the need for actuation by periodic input of thermal energy.

The current results show the possibility to apply time-resolved mass spectrometry in the monitoring of chemical waves. In this demonstration, a relatively low temporal resolution (seconds) was sufficient to observe the between the passive transduction and reaction front. While in previous work we applied optical and mass spectrometric detection in the monitoring of a convection process,[14] here time-resolved mass spectrometry[10] was successfully used to show the difference in the migration speed of chemical waves due to bioautocatalytic reaction and accompanying non-chemical processes.

Modelling biological and chemical processes has been of interest to many scholars. Relevant insights on spatially and temporally resolved processes (such as oscillating reactions) were presented by Arthur Winfree.[15] It might be of potential interest to study the bioautocatalytic process described here in view of the published models of reaction diffusion systems, such as Kolmogorov–Petrovsky–Piskounov's[5] or Fisher's[6] equation. With such models one could potentially disentangle the contributions of enzymatic reaction and passive dispersion of molecules on the propagation of the moving front of ADP/ATP. However, the current experimental setup has limitations that preclude the use of data in quantitative analysis required to study the mechanism of the chemical wave induced by the bioautocatalytic process. This is due to: (i) the use of an ambient ionization system without separation of analytes; (ii) presence of various components (*e.g.* buffer salt) in the aqueous reaction mixture; (iii) the use of ion trap mass analyzer; (iv) formation of a temperature gradient in front of the mass spectrometer's orifice. Overcoming these drawbacks in future should augment quantitative capabilities of the spatiotemporal monitoring by time-resolved mass spectrometry. However, it is also appealing to implement other detection system when quantitative information is required: for example, fluorescence resonance energy transfer probes,[16] immobilized on the wall of the drift cell. Nonetheless, such optical assays would eliminate the possibility of using isotopic labels to distinguish between the trigger ATP and the ATP produced in the course of the reaction. Therefore, in future studies, it would be interesting to use both mass spectrometry as well as optical detection systems as complementary tools.

In summary, the above results show the possibility of transmitting a chemical signal (ADP/ATP) over the range of centimetres with a speed exceeding that of other transport phenomena occurring under the same conditions. We believe the chemical wave propagating ADP and ATP (the energy carriers in biochemistry) can act as a turn-on/off trigger, and be used to initiate various processes in bioengineered systems incorporating tissues, cells, (bio)nanorobots, or various biocatalysts (*e.g.* kinases). Coupling this scheme with other biomolecular constructs (*e.g.* enzyme systems supplying the AMP and PEP substrates) and microfluidics (*e.g.* parallel capillary channels), and using anti-convective media (*e.g.* hydrogels), may further enable multiplexed transmission of binary data. Since the speed of chemical waves – propagating according to the proposed scheme – is related to the kinetic properties of the enzymes involved in the bienzymatic process (*cf.* Fig. S1†), modification of these enzymes (for example, through directed evolution), or taking advantage of non-enzymatic amplification schemes,[17] might further increase the speed of wave propagation, which would augment practicality of this approach for real-world applications.

Acknowledgements

We thank the National Science Council of Taiwan and the National Chiao Tung University for the financial support of this work.

Notes and references

1 R. G. A. Safranyos and S. Caveney, *J. Cell Biol.*, 1985, **100**, 736.
2 Y. Shafrir, D. ben-Avraham and G. Forgacs, *J. Cell Sci.*, 2000, **113**, 2747.
3 F. Wang, H. Wang, J. Wang, H.-Y. Wang, P. L. Rummel, S. V. Garimella and C. Lu, *Biotechnol. Bioeng.*, 2008, **100**, 150.
4 C.-H. Chen and J. G. Santiago, *J. Microelectromech. Syst.*, 2002, **11**, 672.

5 A. Kolmogorov, I. Petrovsky and N. Piskunov, *Moscow Bull. Univ. Math.*, 1937, **1**, 1.
6 R. A. Fisher, *Ann. Eugenics*, 1937, **7**, 355.
7 C. Almarcha, P. M. J. Trevelyan, P. Grosfils and A. De Wit, *Phys. Rev. Lett.*, 2010, **104**, 044501.
8 E. Valero, R. Varón and F. García-Carmona, *Biochem. J.*, 2000, **350**, 237.
9 P. L. Urban, A. Amantonico, S. R. Fagerer, P. Gehrig and R. Zenobi, *Chem. Commun.*, 2010, **46**, 2212.
10 Y.-C. Chen and P. L. Urban, *Trends Anal. Chem.*, 2013, **44**, 106.
11 V. G. Santos, T. Regiani, F. F. G. Dias, W. Romão, J. L. P. Jara, C. F. Klitzke, F. Coelho and M. N. Eberlin, *Anal. Chem.*, 2011, **83**, 1375.
12 A. N. Zaikin and A. M. Zhabotinsky, *Nature*, 1970, **225**, 535.
13 R. K. Saiki, S. Scharf, F. Faloona, K. B. Mullis, G. T. Horn, H. A. Erlich and N. Arnheim, *Science*, 1985, **230**, 1350.
14 P.-H. Li, H. Ting, Y.-C. Chen and P. L. Urban, *RSC Adv.*, 2012, **2**, 12431.
15 A. T. Winfree, *The Geometry of Biological Time*, Springer-Verlag, New York, 2010.
16 H. Imamura, K. P. H. Nhat, H. Togawa, K. Saito, R. Iino, Y. Kato-Yamada, T. Nagai and H. Noji, *Proc. Natl. Acad. Sci. U. S. A.*, 2009, **106**, 15651.
17 X. Chen, N. Briggs, J. R. McLain and A. D. Ellington, *Proc. Natl. Acad. Sci. U. S. A.*, 2013, **110**, 5386.